40-Gb/s Optical Packet Clock Recovery With Simultaneous Reshaping Using a Traveling-Wave Electroabsorption Modulator-Based Ring Oscillator

Zhaoyang Hu, Kohsuke Nishimura, Hsu-Feng Chou, Lavanya Rau, Masashi Usami, John E. Bowers, *Fellow, IEEE*, and Daniel J. Blumenthal, *Fellow, IEEE*

***Abstract*—An injection-locking traveling-wave electroabsorption modulator-based ring oscillator is demonstrated to perform optical clock recovery and simultaneous reshaping of 40-Gb/s optical packets. The transient response analysis and experimental results show strong injection and short loop length reduce the locking time to within 0.3 μs. The recovered packet optical clock has 532-fs timing jitter.**

***Index Terms*—Clock recovery, optical data processing, packet switching, regeneration.**

I. Introduction

OPTICAL packet switching is a promising technique to exploit the flexibility of Internet protocol in optical networks [1]. One challenging key function is optical clock recovery (OCR) from asynchronously arriving packets. Conventional phase-locked loop circuits require several ten microseconds to recover the clock. Previously, self-pulsating distributed feedback lasers and Fabry–Pérot filters have been applied for OCR on a packet-per-packet basis [2], [3]. In our previous work, we demonstrated a novel technique to recover 40-GHz optical clock with 0.5-ps timing jitter and 8-ps pulsewidth in a nonpacket environment. This technique employs a traveling-wave electroabsorption modulator (TW-EAM)-based ring oscillator [4]. A phase shifter was not used and the loop phase was tuned by adjusting TW-EAMs bias due to nonlinear photocurrent generation. The main advantages of this OCR are its simple configuration for potentially monolithic integration as well as simultaneous output of optical data and recovered pulsed optical clocks for subsequent retiming, reshaping, and reamplification regeneration. This technique allows hybrid integration to reduce the loop length to $\sim$18 mm [5].

In this letter, we analyze the characteristics of the OCR reported in [4] for packet switching applications. The clock component of input 40-Gb/s optical packets is detected from the photocurrent of a TW-EAM and extracted by a chip coplanar Q filter ribbon-bonded to the TW-EAM shown as Fig. 1. A 38–40-GHz radio frequency (RF) amplifier is connected to the TW-EAM and Q filter with external RF cables to construct the ring oscillator. A 20-dB RF Monitor T is used in the loop to tap out 40-GHz recovered electrical clock for the measurement of the OCRs locking time. The OCR can be injection locked when input optical packets contain a frequency within its locking range. Recovered electrical clock in the loop is applied on lower electrical port of the TW-EAM to modulate CW light at another wavelength. The modulation effect performs reshaping and retiming due to narrow synchronized TW-EAMs switch window [6]. As shown in Fig. 1, recovered 40-GHz optical clock is synchronized or not synchronized to input optical packets depending on the existence of optical packets or interval gaps.

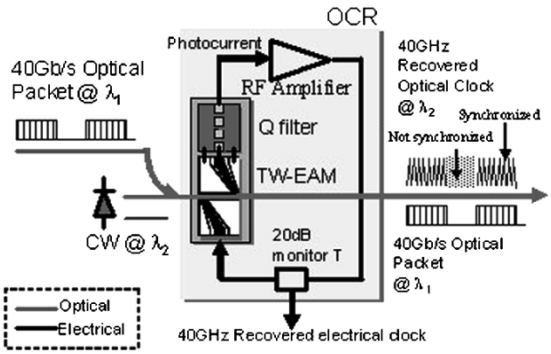

Fig. 1. 40-Gb/s optical packet clock recovery.

II. Transient Response

Injection locking of the ring oscillator-based OCR is used to synchronize the frequency and phase. The output phase ϕ with an injected signal is given by Adler's equation [7]

$$\frac{d\phi}{dt} = \sqrt{\frac{P_{\rm inj}}{P_0}}\frac{\omega_0}{2Q}\sin(\phi) + \Delta\omega_0 \tag{1}$$

where $\Delta\omega_0 = \omega_0 - \omega_{\rm inj}$, ω_0 and $\omega_{\rm inj}$ are frequencies of free-running oscillation and injection signal, respectively; P_0 and $P_{\rm inj}$ are power intensities of free-running oscillation signal and injection signal, respectively; and Q is the quality factor of the oscillator.

The transient response of the oscillator describes its dynamic evolution when the locking signal is injected into the free-running oscillator. For simplicity, we assume the case of $\Delta\omega_0 = 0$ when free-running oscillation frequency is the same as that of

Manuscript received May 17, 2004; revised July 20, 2004. This work was supported by KDDI Grant 442530-59406 and by a State of California UC Discovery Grant 597095-19929.

Z. Hu, H.-F. Chou, L. Rau, J. E. Bowers, and D. J. Blumenthal are with the Department of Electrical and Computer Engineering, University of California, Sanata Barbara, CA 93106-9560 USA (e-mail: huby@ece.ucsb.edu).

K. Nishimura and M. Usami are with KDDI R&D Laboratories, Inc., Saitama 356-8502, Japan.

Digital Object Identifier 10.1109/LPT.2004.836346

1041-1135/04$20.00 © 2004 IEEE

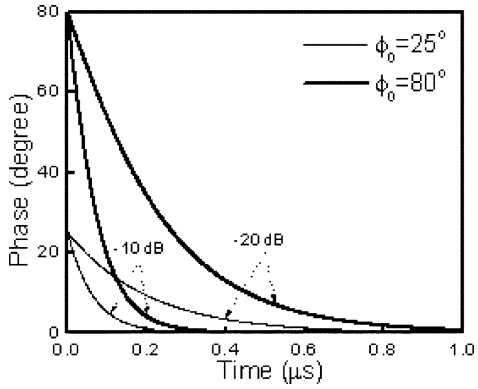

Fig. 2. Transient response of the injection-locked OCR for $\phi_0 = 25°$, 80°, and $P_{\rm inj}/P_0 = -10$ dB, -20 dB, respectively ($P_0 = 10$ dBm, $\tau = 1$ ns, $G = 25$ dB, $\rho = 10^{-17}$ mW/Hz).

locking signal but with an initial phase difference ϕ_0. By integrating (1) for ϕ [8]

$$\int_{\phi_0}^{\phi} \frac{d\phi}{\sin(\phi)} = \sqrt{\frac{P_{\rm inj}}{P_0}}\frac{\omega_0}{2Q}\int_0^t dt \tag{2}$$

which leads directly to

$$\phi(t) = 2\tan^{-1}\left(\exp\left(-\sqrt{\frac{P_{\rm inj}}{P_0}}\frac{\omega_0}{2Q}t\right)\tan\frac{\phi_0}{2}\right) \tag{3}$$

where Q can be defined as the ratio of center oscillation frequency f_0 and its full-width of half-maximum $\Delta f_{\rm FWHM}$ [9]

$$Q = \frac{f_0}{\Delta f_{\rm FWHM}} = 2\pi f_0 \tau^2 \frac{P_0}{\rho G} \tag{4}$$

where τ is the loop delay time, ρ is equivalent input noise density, and G is the power gain. Fig. 2 is a plot of the phase response for different initial phases of ϕ_0 at different injection ratio of $P_{\rm inj}/P_0$ based on estimated parameters. It is seen that smaller initial phase and stronger injection ratio suggest a faster evolution process to the steady state, i.e., shorter locking time.

III. Experimental Results

A 10-GHz gain-switched distributed Bragg reflector (DBR) laser was used to generate pulses at 1555 nm (λ_1) and modulated with $2^{31} - 1$ pseudorandom binary sequence pattern through a $LiNbO_3$ modulator. Optical packets were generated by an acoustooptical modulator and then optically multiplexed to 40 Gb/s. The continuous-wave (CW) light input for generating the recovered optical clock was 6 dBm at 1551 nm (λ_2).

Without an optical signal input, the OCR oscillated at the frequency of 38.858 GHz that is determined by the peak frequency of Q filter and total loop delay, as shown as the inset picture in Fig. 3(a). The bit rate of input optical packets is set to 38.8576 Gb/s within the locking range of the OCR. When the optical packets and CW light inject to the OCR, both clock component and free-running mode exist in the loop, as shown in Fig. 3(a). By adjusting the reverse bias of the TW-EAM to 0.86 V, the OCR oscillation frequency was tuned close to the input signal and its phase was also locked, as shown in Fig. 3(b). The sidebands in the RF spectrum of the injection-locked OCR

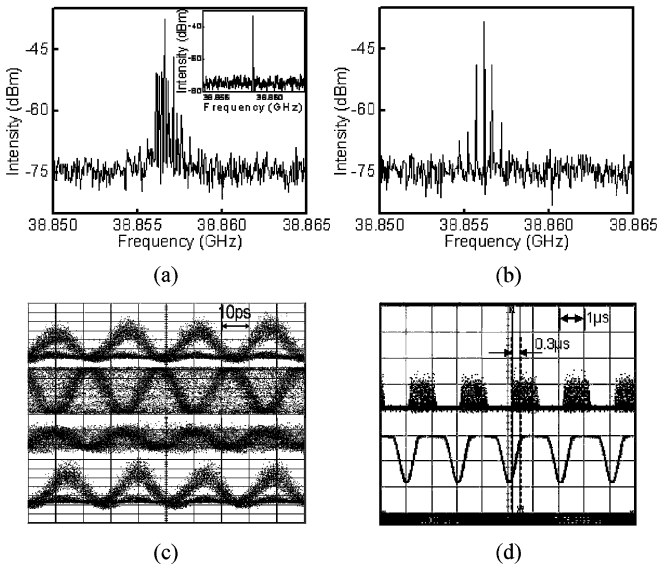

Fig. 3. (a) RF spectrum before injection locking. Inset: Free-running OCR. (b) RF spectrum after injection locking. (c) Eye diagrams of input ~40-Gb/s optical packets, recovered ~40-GHz electrical and optical clocks, and output ~40-Gb/s optical packets, respectively. (d) Input optical packets (upper) and output IF signal from the mixer (lower).

are generated from low frequency modulation characteristics of optical packets. The eye diagrams of input ~40-Gb/s optical packets, recovered ~40-GHz electrical and optical clocks, and output ~40-Gb/s optical packets are shown one by one from the top waveform in Fig. 3(c), respectively. The overlap of synchronized and not synchronized clock signals, corresponding to optical packets and interval gaps, lead to smeared pictures due to the sampling nature of the oscilloscope. The TW-EAM introduced 17-dB insertion loss mainly from coupling loss. It can be reduced by carefully matching the mode shapes of TW-EAM and lensed fibers.

An RF mixer is used to measure the OCR's locking time. A ~10-GHz RF signal from the transmitter is electrically multiplexed to ~40-GHz RF signal and enters the local oscillator port of the mixer; recovered ~40-GHz electrical clock from Monitor T goes to the RF port of the mixer. The output intermediate frequency (IF) signal from the mixer is shown as the lower waveform in Fig. 3(d). The locking time is measured from arrival time of optical packets to that of clock buildup. A 0.3-μs locking time was measured in 0.3-m loop length. When average power of input optical packets was reduced from 3 to -2 dBm, locking time is increased from 0.3 to 1.2 μs [shown as the scattered dots in Fig. 4(a)]. Assuming 1) 10% power of input optical signal is converted and injected to the OCR and 2) injected signal power is twice the average power due to 50/50 duty cycle of input packets and gaps, we approximately simulate the relationship between locking time and different input average power, shown as the solid curve in Fig. 4(a). The experimental results follow the tendency but are not well matched. We believe the reason is due to uncertain initial phase difference in the experiment when changing the measurement conditions, but assuming fixed initial phase in the simulation. The influence of the OCRs loop delay time on locking time is also simulated and measured, both shown as solid curve and scattered dots in Fig. 4(b), respectively. Locking time was reduced from 2 to 0.3 μs when shortening the OCR's loop length from 1.28 to 0.3 m. The OCR's holding

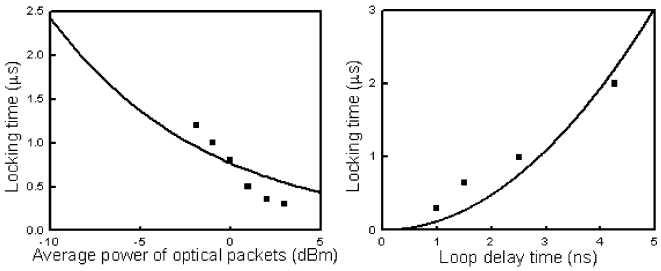

Fig. 4. Locking time against (a) average power of input ∼40-Gb/s optical packets and (b) the OCR's loop delay time (solid curves: simulation results; scattered dots: experimental results).

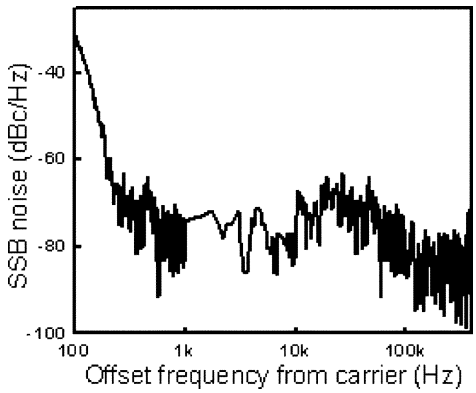

Fig. 5. SSB noise spectrum of recovered optical clock (resolution bandwidth: 100 Hz).

time is also measured, i.e., how long the clock will stay synchronized to data after dropping injected signal. We found the holding time keeps ∼0.4 μs for different injection power from −2 to 3 dBm, while it increases to 2 μs when the loop length increases to 1.28 m. Shorter locking time and holding time can be achieved by integrating the OCR on the same platform so as to minimize the loop length to several millimeters, which corresponds to several-nanosecond-locking time. In addition, increasing the loop gain or reducing the loop loss can decrease the locking time based on (3) and (4).

Fig. 5 depicts single sideband (SSB) noise spectrum of the main peak of recovered ∼40-GHz optical clock (with erbium-doped fiber amplification). We obtained the root-mean-square jitter of 532 fs through integrating the noise spectrum from offset frequency of 100 Hz to 400 kHz. Above 400-kHz offset frequency, first sideband occurs due to low frequency modulation of the optical packet clocks. The jitter mainly comes from input signal because the OCR follows the input signal's jitter within the locking range and suppresses the jitter outside the locking range [4].

To demonstrate the OCR's reshaping capability, the pulsewidth from the gain-switched DBR laser was intentionally broadened from 10 to 18 ps. As shown in Fig. 6, the data signal was reshaped due to less than 10-ps TW-EAM's switch window when comparing the eye diagrams of output and input optical packets. Also, less timing jitter can be achieved under the narrow synchronized window. Comparing recovered

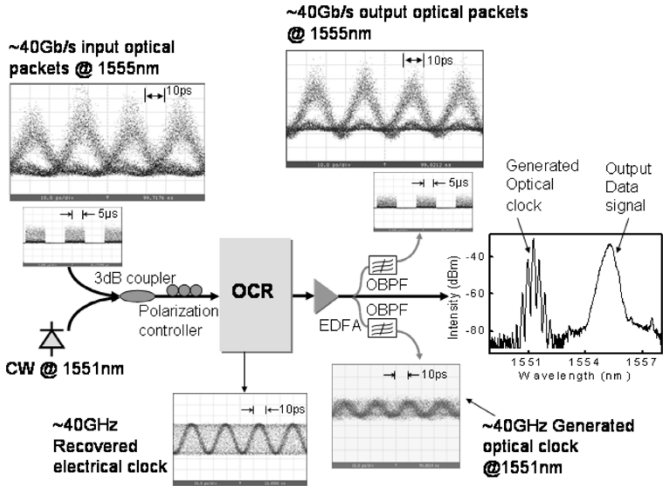

Fig. 6. Simultaneous clock recovery and reshaping.

clocks from the cases of narrow pulses and broadened pulses, no obvious differences were observed. Successful operation of the OCR is only determined by the clock tone of input signals.

IV. Conclusion

OCR and simultaneous reshaping for 40-Gb/s optical packets has been demonstrated for the first time by utilizing an OCR consisting of a TW-EAM-based ring oscillator. The OCR achieves clock recovery within 0.3 μs and the recovered optical clock has 532-fs timing jitter. Transient response analysis and experimental results show that an OCR with strong injection power and short loop length is desired for fast locking time.

References

[1] A. Carena, M. D. Vaughn, R. Gaudino, M. Shell, and D. J. Blumenthal, "OPERA: An optical packet experimental routing architecture with label swapping capability," *J. Lightwave Technol.*, vol. 16, pp. 2135–2145, Dec. 1998.

[2] B. Sartorius, C. Bornholdt, S. Bauer, and M. Mohrle, "40 GHz optical clock recovery for application in asynchronous networks," in *Eur. Conf. Optical Communication (ECOC)*, 2001, Paper We.P.3.2, pp. 442–443.

[3] N. Pleros, K. Vyrsokinos, C. Bintjas, K. Yiannopoulos, K. Vlachos, H. Avramopoulos, and G. Guekos, "All-optical clock recovery from short asynchronous data packets at 10 Gb/s," *IEEE Photon. Technol. Lett.*, vol. 15, pp. 1291–1293, Sept. 2003.

[4] Z. Hu, H.-F. Chou, J. E. Bowers, and D. J. Blumenthal, "40-Gb/s optical clock recovery using a compact traveling-wave electroabsorption modulator-based ring oscillator," *IEEE Photon. Technol. Lett.*, vol. 16, pp. 1376–1378, May 2004.

[5] Z. Hu, B. Liu, X. Yan, J. E. Bowers, and D. J. Blumenthal, "All-optical 40 Gb/s cross-wavelength transferred clock recovery for 3R wavelength conversion using a traveling-wave electroabsorption modulator-based resonant cavity," in *Optical Fiber Communication Conf. on CD-ROM*, Washington, DC, 2004, Paper WD3.

[6] K. Nishmura, M. Tsurusawa, and M. Usami, "Novel all-optical 3R regenerator using cross-absorption modulation in RF-driven electroabsorption waveguide," in *Eur. Conf. Optical Communication (ECOC)*, 2001, Paper We.F.2.4, pp. 286–287.

[7] R. Adler, "A study of locking phenomenon in oscillators," *Proc. IEEE*, vol. 61, pp. 1380–1385, Oct. 1973.

[8] K. Kurokawa, "Injection locking of microwave solid-state oscillators," *Proc. IEEE*, vol. 61, pp. 1386–1410, Oct. 1973.

[9] X. S. Yao and L. Maleki, "Optoelectronic microwave oscillator," *J. Opt. Soc. Amer. B*, vol. 13, pp. 1725–1735, 1996.